DNA origami based superconducting nanowires

Lior Shani, Philip Tinnefeld, Yafit Fleger, Amos Sharoni, Boris Ya. Shapiro, Avner Shaulov, Oleg Gang, and Yosef Yeshurun

COLLECTIONS

Paper published as part of the special topic on Chemical Physics, Energy, Fluids and Plasmas, Materials Science and Mathematical Physics

F This paper was selected as Featured

DNA origami based superconducting nanowires Ⓕ
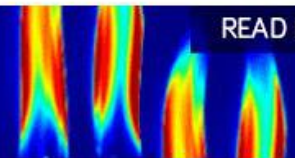
View Online   Export Citation   CrossMark

Lior Shani,[1,2,a] �� Philip Tinnefeld,[3] Yafit Fleger,[2] Amos Sharoni,[1,2] �� Boris Ya. Shapiro,[1] Avner Shaulov,[1,2]
Oleg Gang,[4,5,6] ⦿ and Yosef Yeshurun[1,2] ⦿

AFFILIATIONS

[1] Department of Physics, Bar-Ilan University, 5290002 Ramat-Gan, Israel

[2] Bar-Ilan Institute of Nanotechnology and Advanced Materials (BINA), 5290002 Ramat-Gan, Israel

[3] Department of Chemistry and Center for NanoScience, Ludwig-Maximilians-Universität München, Butenandtstr. 5-13,
 81377 München, Germany

[4] Department of Applied Physics and Applied Mathematics, Columbia University, New York, New York 10027, USA

[5] Department of Chemical Engineering, Columbia University, New York, New York 10027, USA

[6] Center for Functional Nanomaterials, Brookhaven National Laboratory, Upton, New York 11973, USA

[a] Author to whom correspondence should be addressed: Lior.shani@biu.ac.il

ABSTRACT

Utilizing self-assembled DNA structures in the development of nanoelectronic circuits requires transforming the DNA strands into highly conducting wires. Toward this end, we investigate the use of DNA self-assembled nanowires as templates for the deposition of a superconducting material. Nanowires formed by the deposition of superconducting NbN exhibit thermally activated and quantum phase slips as well as exceptionally large negative magnetoresistance. The latter effect can be utilized to suppress a significant part of the low temperature resistance caused by the quantum phase slips.

The continuing quest for reducing the size of electronic components has led to the emergence of a new field of research, aiming at the study and application of molecular building blocks for the fabrication of electronic components.[1–4] In this ambitious endeavor, DNA molecules are expected to play an important role. The unique ability of DNA to self-assemble[5] into arbitrary structures[6–12] suggests its use as a network on which various molecular electronic components can be placed.[13–15] For this purpose, numerous metallization processes have been attempted aiming to transform DNA molecules[2,16] and DNA origami[13–15] into electrically conducting wires. Various metals have been employed, including silver,[17] palladium,[18] and gold.[19] The reported resistance values have spanned over several orders of magnitude, typically in the range of $10^2 \ \Omega$–$10^6 \ \Omega$.[16] To increase conductivity, superconducting materials were used to fabricate superconducting nanowires, using molecules such as carbon nanotubes[20–22] and DNA[22,23] as templates. There are, however, no reports in the literature describing superconducting nanowires that use DNA *origami* as a template. The flexibility of DNA origami can be used as a powerful technique for fabrication of complex shaped nano-objects[9–12] that can be converted

into functional superconducting devices, hence motivating the study of the physical properties of DNA origami based superconducting nanowires.

Here, we investigate the use of DNA self-assembled nanowires as templates for the deposition of superconducting NbN. We demonstrate coating self-assembled DNA nanowires with superconducting NbN and report on magneto-transport properties of the resulting nanowires. Due to the nanometric lateral size of these nanowires, their resistance does not drop to zero as temperature drops below the superconducting transition temperature, T_c. This well-known phenomenon has been observed in studies of various superconducting nanowires and has been ascribed to thermally activated phase slips (TAPSs) near T_c and to quantum phase slips (QPSs) far below T_c (for a review, see Ref. 24). The NbN nanowires also show exceptionally large negative magnetoresistance (NMR) that can be utilized to reduce a significant part of the low temperature resistance resulting from the QPS.

DNA origami nanowires were prepared as described previously in detail.[25] A typical TEM image of the resulting DNA origami nanowires is shown in Fig. 1(a), revealing ~220 nm long and
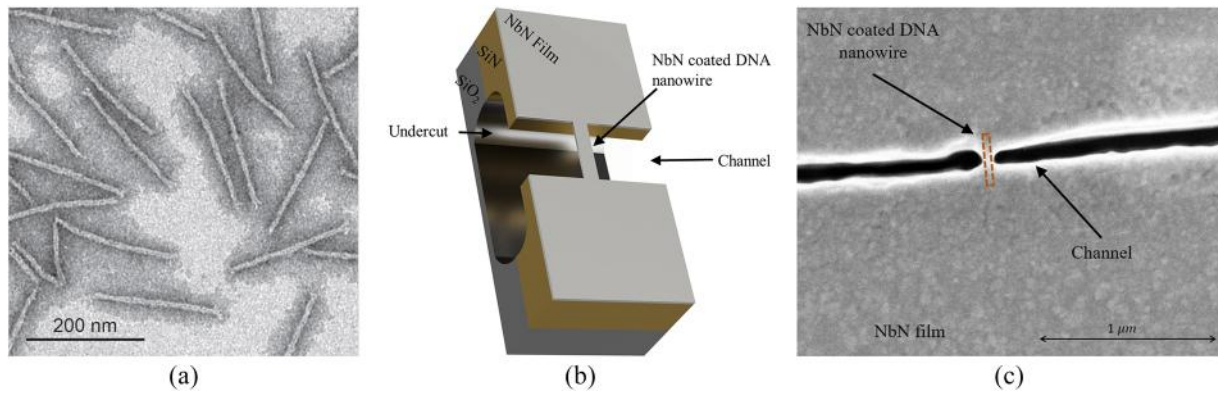
FIG. 1. (a) TEM image of DNA origami nanowires before coating. (b) Schematic illustration of an NbN coated DNA nanowire suspended above a SiN/SiO$_2$ channel. (c) HR-SEM image of the channel (black) on which the DNA nanowire is suspended. In the image, the channel appears discontinuous reflecting the DNA nanowire suspended across it (marked by the orange dashed rectangle). The distance between the two sides of the channel is ~50 nm, and the width of the NbN coated DNA nanowire at its narrowest point is ~25 nm.

~15 nm wide wires. The DNA origami nanowires were drop-casted on a SiN/SiO$_2$ chip with a ~50 nm wide channel, as schematically shown in Fig. 1(b). The channel was prepared using e-beam lithography followed by CHF$_3$–H$_2$ Reactive Ion Etching (Plasma-Therm, RIE) to remove ~25 nm layer of SiN. In order to prevent shortcuts in the electrical measurements after NbN deposition, a ~200 nm deep and ~170 nm wide undercut was formed in SiO$_2$ by wet etching, using hydrofluoric acid (HF). The chip with the DNA nanowires was dried for 12 h in vacuum and then coated with ~10 nm layer of NbN, using the AJA magnetron sputtering system. The chamber pressure was kept at 1.7 mTorr to avoid clustering of NbN during the sputtering process.

Figure 1(c) shows an HR-SEM image of the channel (black) with the DNA wire laid on it. The NbN coated wire and substrate are shown in bright gray color. The location of the DNA wire (which is coated with NbN and, therefore, cannot be seen in the image) is shown schematically by the orange dashed rectangle. The width of the wire after NbN deposition is ~25 nm at its narrowest point, and as can be seen, it changes along its length. In the range of ~30 nm, the change in the width is only few nm. In the following, the effective length of the DNA wire is taken as 30 nm.

To measure the transport properties of a single DNA nanowire, we patterned a four-probe setup on the NbN coated film, using negative tone photolithography (MLA Heidelberg Inst.), followed by Cl$_2$–BCl$_3$ etching to remove NbN around the pads and the channel. In addition, we disconnected excess DNA wires along the channel using the helium ion beam (Orion Nanolab, Zeiss), which is nondestructive to the superconducting layer.[26]

The magneto-transport properties of the NbN coated DNA nanowire were measured using the Physical Property Measuring System (PPMS, Quantum Design). Figure 2 shows the temperature dependence of the resistance of the NbN nanowire at zero field (blue line), demonstrating a superconducting transition at T$_c$ ~ 5 K, lower as compared to that measured in the bulk (~16 K[27]); a reduction in T$_c$ is commonly observed in nanowires and ascribed to degradation and oxidation of the superconducting material during the fabrication process (see, e.g., Refs. 28 and 29). The observed

broadening of the transition is associated with thermally activated phase slips (TAPS), the theory of which was developed by Langer, Ambegaokar, McCumber, and Halperin Refs. 30 and 31. From this theory, assuming that the order parameter $\Delta = \Delta_0 (1 - T/T_c)^{1/2}$, one can derive[32] the following expression for the resistance in the TAPS region below T$_c$:

$$R(t) = R_0 \frac{(1-t)^{1/2}}{t^2} \exp\left(-\frac{\gamma_{TAPS}\sqrt{1-t}}{t}\right), \qquad (1)$$

where $t = T/T_c$ and $\gamma_{TAPS} = N(\varepsilon_F)\Delta_0^2 \xi_0 S/2T_c$, in which $N(\varepsilon_F)$ is the density of states at the Fermi level and S is the cross section of the wire. The red dotted line in Fig. 2 shows a fit of Eq. (1) to the experimental data, taking R_0 and γ_{TAPS} as fitting parameters, yielding $R_0 = 5 \cdot 10^4 \ \Omega$ and $\gamma_{TAPS} = 7$. This value of γ_{TAPS} corresponds to the estimated value calculated using common experimental values for NbN:[33] $N(\varepsilon_F) \approx 10^{-1}$states/eV, $\Delta_0 = 88$ meV, $\xi_0 = 5$ nm, and $T_c = 5$ K, and assuming that S ~ 140 nm^2. This value of S is somewhat smaller than the measured one, suggesting the presence
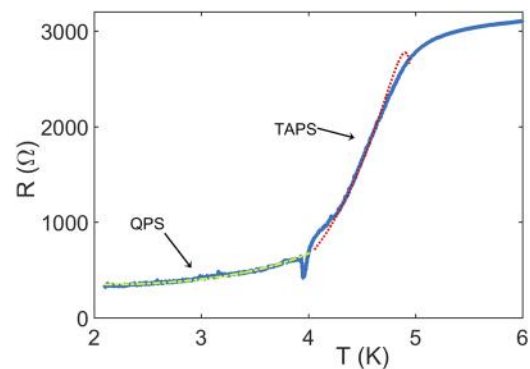

FIG. 2. Resistance as a function of temperature (blue line), measured at zero field. The red dotted line is a fit to Eq. (1), and the green dashed line is a fit to Eq. (2).

of an oxidation layer of ~2 nm, consistent with the value reported in Ref. 34. Apparently, Eq. (1) yields a good fit to the data in the range ~4 K to 5 K, but it fails at low temperatures where the resistance shows a "tail" with a weak temperature dependence. This resistance tail is attributed to the combined effect of quantum phase slips and charge imbalance.[35,36] Taking into account these two contributions, one can derive[32] the following expression for the temperature dependence of the resistance in the QPS regime:

$$R(t) = R_0^* t^{-3/2} (1-t)^{1/4} \exp\left(-\gamma_{QPS}(1-t)^{1/2}\right). \quad (2)$$

Here, $\gamma_{QPS} = A \frac{h}{4e^2 R_N} \frac{L}{\xi_0}$, where A is of order 1, $L = 30$ nm is the effective length of the wire, and $R_N = 3000\ \Omega$ is the resistance above the transition temperature. The green dashed line in Fig. 2 exhibits a good fit of Eq. (2) to the low temperature data, yielding $R_0^* = 2 \cdot 10^5\ \Omega$ and $\gamma_{QPS} = 6$. This value of γ_{QPS} implies $A = 0.5$. By passing, we note an unexplained dip in the R(T) data, which separates the TAPS and QPS regimes. A very similar dip was reported earlier.[21]

Figure 3(a) shows the field dependence of the NbN nanowire resistance for temperatures between 2.2 K and 3.7 K, i.e., in the temperature range of the resistance tail. With the increase in the magnetic field, the resistance initially decreases, exhibiting a negative magnetoresistance (NMR), reaching a minimum value at a field

H_{min}, and then continuously increases. The NMR effect is more pronounced as the temperature decreases.

Figure 3(b) shows the size of the effect, measured by the ratio $r = (R(H) - R(0))/R(0)$, as a function of temperature, where $R(0)$ and $R(H)$ are the resistance at zero field and at H_{min}, respectively. The figure also shows the values of H_{min} vs temperature. Apparently, the increase in $|r|$ is accompanied by an increase in H_{min}. Although NMR has been previously reported for various superconducting nanowires, see, e.g., Refs. 37–42, we note that the effect observed here is exceptionally large, reaching a value of ~90% at low temperatures.

The origin of the negative magnetoresistance ($dR/dH < 0$) is commonly associated with quasiparticles' charge imbalance, accompanying each phase slip event that decays in time and space.[36,43] The resistance associated with the charge imbalance is given by[36]

$$R_Q = \frac{\rho_N}{S} \Lambda_Q \tau_0 \Gamma_{PS}, \quad (3)$$

where ρ_N is the resistivity of the normal region, Λ_Q is the charge imbalance decay length, Γ_{PS} is the average rate of the phase slips, and τ_0 is the duration of each event. The charge imbalance decay length, Λ_Q, decreases with the field according to[36]

$$\Lambda_Q = \sqrt{\frac{2DT_c \tau_E}{\pi \Delta}} \left[1 + \frac{3.52 \tau_E T_c}{\hbar} b^2 \right]^{-\frac{1}{4}}, \quad (4)$$

where D is the diffusion constant, τ_E is the electron–phonon inelastic scattering time, and $b = H/H_{c2}$. The magnetoresistance behavior of superconducting nanowires is, thus, governed by two competing processes: rate of phase slips, Γ_{PS}, which increases with the magnetic field due to the suppression of Δ, and charge imbalance decay length, Λ_Q, which decreases with the field. This competition dictates the behavior of the magnetoresistance: At low fields, the decrease in Λ_Q with the field dominates, giving rise to $dR/dH < 0$. At high fields, the increase in Γ_{ps} with the field dominates, giving rise to $dR/dH > 0$. To explain the relatively large NMR effect observed in our NbN nanowires, we note that Γ_{ps} increases with the length of the wire as the probability of a phase slip event increases with the length. However, as is clear from Eq. (4), Λ_Q is independent of the length. Consequently, as the length of the wire increases, the increasing contribution to the total resistance overcomes the decreasing part already at lower fields. Thus, the large NMR in our NbN coated DNA samples is presumably due to the short length of the wires. Indeed, recently reported magnetoresistance measurements in ~ 5μm long NbN wires[41] exhibit a smaller NMR effect, i.e., a maximum reduction of ~30% of the resistance value compared to more than 90% reduction in our measured sample.

In conclusion, this work demonstrates the ability to fabricate superconducting nanowires using DNA origami wires as templates. A similar "bottom-up" approach can be further adopted in fabrication of 2D or 3D superconducting nanostructures,[44] where the conventional "top-bottom" techniques, such as e-beam lithography, show their limitations. The DNA origami based NbN nanowires exhibit properties characteristic of nanowires fabricated using conventional techniques, namely, phase slips and negative magnetoresistance. Nevertheless, the NMR effect exhibited by the NbN coated DNA wires is exceptionally large, a phenomenon that should be further investigated. The results of this work can be used in various
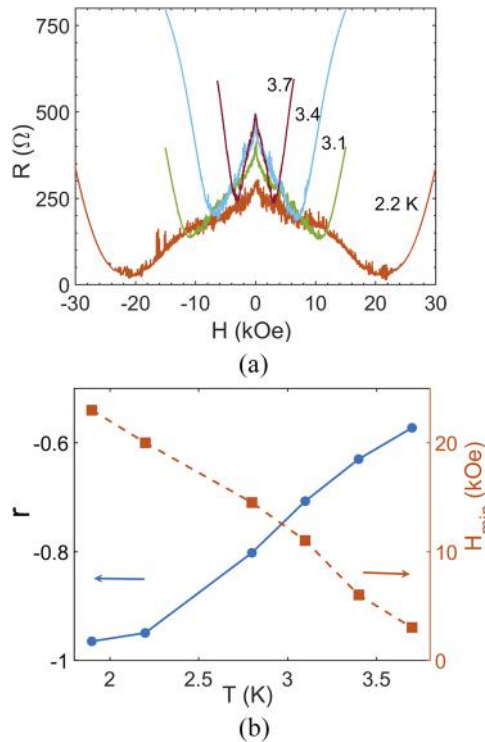
FIG. 3. (a) Resistance as a function of magnetic field at the indicated temperatures. (b) Temperature dependence of the size of the NMR effect, r (blue circles, left ordinate), and the field H_{min} where the minimal resistance is obtained (orange squares, right ordinate) and the lines are guides to the eye.

applications, including interconnects in nano-electronics and novel devices based on exploitation of the flexibility DNA origami in fabrication of 3D architectures, e.g., 3D SQUIDs[45] for the measurement of the magnetic field vector.

DATA AVAILABILITY

The data that support the findings of this study are available from the corresponding author upon reasonable request.

REFERENCES

[1] A. Csáki, G. Maubach, D. Born, J. Reichert, and W. Fritzsche, "DNA-based molecular nanotechnology," Single Mol. **3**, 275–280 (2002).

[2] E. Braun and K. Keren, "From DNA to transistors," Adv. Phys. **53**, 441–496 (2004).

[3] M. G. Warner and J. E. Hutchison, "Linear assemblies of nanoparticles electrostatically organized on DNA scaffolds," Nat. Mater. **2**, 272–277 (2003).

[4] K. Keren, R. S. Berman, E. Buchstab, U. Sivan, and E. Braun, "DNA-templated carbon nanotube field-effect transistor," Science **302**, 1380–1382 (2003).

[5] P. W. K. Rothemund, "Folding DNA to create nanoscale shapes and patterns," Nature **440**, 297 (2006).

[6] M. Siavashpouri, C. H. Wachauf, M. J. Zakhary, F. Praetorius, H. Dietz, and Z. Dogic, "Molecular engineering of chiral colloidal liquid crystals using DNA origami," Nat. Mater. **16**, 849–856 (2017).

[7] H. Jun, F. Zhang, T. Shepherd, S. Ratanalert, X. Qi, H. Yan, and M. Bathe, "Autonomously designed free-form 2D DNA origami," Sci. Adv. **5**, eaav0655 (2019).

[8] Y. Tian, J. R. Lhermitte, L. Bai, T. Vo, H. L. Xin, H. Li, R. Li, M. Fukuto, K. G. Yager, and J. S. Kahn, "Ordered three-dimensional nanomaterials using DNA-prescribed and valence-controlled material voxels," Nat. Mater. **19**, 789 (2020).

[9] W. Liu, M. Tagawa, H. L. Xin, T. Wang, H. Emamy, H. Li, K. G. Yager, F. W. Starr, A. V. Tkachenko, and O. Gang, "Diamond family of nanoparticle superlattices," Science **351**, 582–586 (2016).

[10] C. Tian, M. A. L. Cordeiro, J. Lhermitte, H. L. Xin, L. Shani, M. Liu, C. Ma, Y. Yeshurun, D. DiMarzio, and O. Gang, "Supra-nanoparticle functional assemblies through programmable stacking," ACS Nano **11**, 7036–7048 (2017).

[11] T. Gerling, K. F. Wagenbauer, A. M. Neuner, and H. Dietz, "Dynamic DNA devices and assemblies formed by shape-complementary, non–base pairing 3D components," Science **347**, 1446–1452 (2015).

[12] D. Han, S. Pal, J. Nangreave, Z. Deng, Y. Liu, and H. Yan, "DNA origami with complex curvatures in three-dimensional space," Science **332**, 342–346 (2011).

[13] B. Uprety, T. Westover, M. Stoddard, K. Brinkerhoff, J. Jensen, R. C. Davis, A. T. Woolley, and J. N. Harb, "Anisotropic electroless deposition on DNA origami templates to form small diameter conductive nanowires," Langmuir **33**, 726–735 (2017).

[14] A. C. Pearson, J. Liu, E. Pound, B. Uprety, A. T. Woolley, R. C. Davis, and J. N. Harb, "DNA origami metallized site specifically to form electrically conductive nanowires," J. Phys. Chem. B **116**, 10551–10560 (2012).

[15] B. R. Aryal, T. R. Westover, D. R. Ranasinghe, D. G. Calvopiña, B. Uprety, J. N. Harb, R. C. Davis, and A. T. Woolley, "Four-point probe electrical measurements on templated gold nanowires formed on single DNA origami tiles," Langmuir **34**, 15069–15077 (2018).

[16] T. Bayrak, N. Jagtap, and A. Erbe, "Review of the electrical characterization of metallic nanowires on DNA templates," Int. J. Mol. Sci. **19**, 3019 (2018).

[17] S. H. Park, M. W. Prior, T. H. LaBean, and G. Finkelstein, "Optimized fabrication and electrical analysis of silver nanowires templated on DNA molecules," Appl. Phys. Lett. **89**, 033901 (2006).

[18] J. Lund, J. Dong, Z. Deng, C. Mao, and B. A. Parviz, "Electrical conduction in 7 nm wires constructed on λ-DNA," Nanotechnology **17**, 2752 (2006).

[19] A. Ongaro, F. Griffin, P. Beecher, L. Nagle, D. Iacopino, A. Quinn, G. Redmond, and D. Fitzmaurice, "DNA-templated assembly of conducting gold nanowires between gold electrodes on a silicon oxide substrate," Chem. Mater. **17**, 1959–1964 (2005).

[20] A. Bezryadin, C. N. Lau, and M. Tinkham, "Quantum suppression of superconductivity in ultrathin nanowires," Nature **404**, 971–974 (2000).

[21] K. Kato, T. Takagi, T. Tanabe, S. Moriyama, Y. Morita, and H. Maki, "Manipulation of phase slips in carbon-nanotube-templated niobium-nitride superconducting nanowires under microwave radiation," Sci. Rep. **10**, 14278 (2020).

[22] M. Remeika and A. Bezryadin, "Sub-10 nanometre fabrication: Molecular templating, electron-beam sculpting and crystallization of metallic nanowires," Nanotechnology **16**, 1172 (2005).

[23] D. S. Hopkins, D. Pekker, P. M. Goldbart, and A. Bezryadin, "Quantum interference device made by DNA templating of superconducting nanowires," Science **308**, 1762–1765 (2005).

[24] K. Y. Arutyunov, D. S. Golubev, and A. D. Zaikin, "Superconductivity in one dimension," Phys. Rep. **464**, 1–70 (2008).

[25] J. J. Schmied, C. Raab, C. Forthmann, E. Pibiri, B. Wünsch, T. Dammeyer, and P. Tinnefeld, "DNA origami–based standards for quantitative fluorescence microscopy," Nat. Protoc. **9**, 1367 (2014).

[26] B. Müller, M. Karrer, F. Limberger, M. Becker, B. Schröppel, C. Burkhardt, R. Kleiner, E. Goldobin, and D. Koelle, "Josephson junctions and SQUIDs created by focused helium-ion-beam irradiation of YBa₂Cu₃O₇," Phys. Rev. Appl. **11**, 044082 (2019).

[27] B. T. Matthias, T. H. Geballe, and V. B. Compton, "Superconductivity," Rev. Mod. Phys. **35**, 1 (1963).

[28] M. D. Henry, S. Wolfley, T. Young, T. Monson, C. J. Pearce, R. Lewis, B. Clark, L. Brunke, and N. Missert, "Degradation of superconducting Nb/NbN films by atmospheric oxidation," IEEE Trans. Appl. Supercond. **27**, 1–5 (2017).

[29] D. D. Bacon, A. T. English, S. Nakahara, F. G. Peters, H. Schreiber, W. R. Sinclair, and R. B. Van Dover, "Properties of NbN thin films deposited on ambient temperature substrates," J. Appl. Phys. **54**, 6509–6516 (1983).

[30] D. E. McCumber and B. I. Halperin, "Time scale of intrinsic resistive fluctuations in thin superconducting wires," Phys. Rev. B **1**, 1054 (1970).

[31] J. S. Langer and V. Ambegaokar, "Intrinsic resistive transition in narrow superconducting channels," Phys. Rev. **164**, 498 (1967).

[32] B. Y. Shapiro, "Negative magneto-resistance in a long superconducting wires: Theory and experiments," preprint arXiv:2011.04529.

[33] A. A. Abrikosov, *Fundamentals of the Theory of Metals* (Courier Dover Publications, 2017).

[34] A. Darlinski and J. Halbritter, "Angle-resolved XPS studies of oxides at NbN, NbC, and Nb surfaces," Surf. Interface Anal. **10**, 223–237 (1987).

[35] D. Y. Vodolazov, "Negative magnetoresistance and phase slip process in superconducting nanowires," Phys. Rev. B **75**, 184517 (2007).

[36] K. Y. Arutyunov, "Negative magnetoresistance of ultra-narrow superconducting nanowires in the resistive state," Physica C **468**, 272–275 (2008).

[37] X. D. Baumans, D. Cerbu, O.-A. Adami, V. S. Zharinov, N. Verellen, G. Papari, J. E. Scheerder, G. Zhang, V. V. Moshchalkov, and A. V. Silhanek, "Thermal and quantum depletion of superconductivity in narrow junctions created by controlled electromigration," Nat. Commun. **7**, 10560 (2016).

[38] Y. Chen, S. Snyder, and A. Goldman, "Magnetic-field-induced superconducting state in Zn nanowires driven in the normal state by an electric current," Phys. Rev. Lett. **103**, 127002 (2009).

[39] A. Rogachev, T.-C. Wei, D. Pekker, A. Bollinger, P. M. Goldbart, and A. Bezryadin, "Magnetic-field enhancement of superconductivity in ultranarrow wires," Phys. Rev. Lett. **97**, 137001 (2006).

[40]P. Xiong, A. V. Herzog, and R. C. Dynes, "Negative magnetoresistance in homogeneous amorphous superconducting Pb wires," Phys. Rev. Lett. **78**, 927 (1997).

[41]K. Masuda, S. Moriyama, Y. Morita, K. Komatsu, T. Takagi, T. Hashimoto, N. Miki, T. Tanabe, and H. Maki, "Thermal and quantum phase slips in niobium-nitride nanowires based on suspended carbon nanotubes," Appl. Phys. Lett. **108**, 222601 (2016).

[42]S. Mitra, G. C. Tewari, D. Mahalu, and D. Shahar, "Negative magnetoresistance in amorphous indium oxide wires," Sci. Rep. **6**, 37687 (2016).

[43]M. Zgirski, K.-P. Riikonen, V. Touboltsev, and K. Y. Arutyunov, "Quantum fluctuations in ultranarrow superconducting aluminum nanowires," Phys. Rev. B **77**, 054508 (2008).

[44]L. Shani, A. N. Michelson, B. Minevich, Y. Fleger, M. Stern, A. Shaulov, Y. Yeshurun, and O. Gang, "DNA-assembled superconducting 3D nanoscale architectures," Nat. Commun. **11**, 5697 (2020).

[45]M. J. Martínez-Pérez, D. Gella, B. Müller, V. Morosh, R. Wölbing, J. Sesé, O. Kieler, R. Kleiner, and D. Koelle, "Three-axis vector nano superconducting quantum interference device," ACS Nano **10**, 8308–8315 (2016).